

# A local Fock-exchange potential in Kohn-Sham equations

T.W. Hollins<sup>1</sup>, S.J. Clark<sup>1</sup>, K. Refson<sup>2,3</sup> and N.I. Gidopoulos<sup>1</sup>

<sup>1</sup> Department of Physics, Durham University, South Road,  
Durham, DH1 3LE, United Kingdom.

<sup>2</sup>Department of Physics, Royal Holloway, University of London,  
Egham TW20 0EX, United Kingdom.

<sup>3</sup>ISIS Facility, Science and Technology Facilities Council,  
Rutherford Appleton Laboratory, Didcot OX11 0QX, United  
Kingdom.

## Abstract.

We derive and employ a local potential to represent the Fock exchange operator in electronic single-particle equations. This local Fock-exchange (LFX) potential is very similar to the exact exchange (EXX) potential in density functional theory (DFT). The practical software implementation of the two potentials (LFX and EXX) yields robust and accurate results for a variety of systems (semiconductors, transition metal oxides) where Hartree Fock and popular approximations of DFT typically fail. This includes examples traditionally considered qualitatively inaccessible to calculations that omit correlation.

## 1. Introduction

The exchange symmetry in quantum mechanics refers to the invariance of a quantum system when two identical particles exchange positions. For electronic systems in particular, this symmetry leads to Pauli's exclusion principle that makes necessary the use of antisymmetric, or fermionic, wave functions.

However, in the theory of electronic structure, the term “exchange” is often used in the narrower context of an effective description that treats the interacting electrons as independent particles, assigning a spin-orbital ( $\phi_i$ ) to each one of them. The  $N$ -electron system is represented by a Slater determinant ( $\Phi$ ) built on the set of spin-orbitals  $\{\phi_i\}$  and the electrons do not interact directly with each other but each electron lies in the effective field of the other  $N - 1$  electrons. The two principal examples of such effective, independent-particle descriptions are the Hartree-Fock (HF) approximation [1] and the Kohn-Sham (KS) scheme [2] in density functional theory (DFT) [3]. Based on the reference state  $\Phi$  of the model, the definition of the exchange energy is given in the context of such an independent-particle theory,

$$E_x[\Phi] = -\frac{1}{2} \sum_{\sigma} \int \int d\mathbf{r} d\mathbf{r}' \frac{|\rho_{\Phi}^{\sigma}(\mathbf{r}, \mathbf{r}')|^2}{|\mathbf{r} - \mathbf{r}'|}. \quad (1)$$

where  $\rho_{\Phi}^{\sigma}(\mathbf{r}, \mathbf{r}')$  with  $\sigma = \uparrow, \downarrow$  is the one-particle reduced density matrix of the reference Slater determinant  $\Phi$ .

Hence, the exchange energy is defined differently in HF theory, where  $\Phi$  is the HF Slater determinant  $\Phi_{\text{HF}}$ , from DFT where  $\Phi$  is the KS Slater determinant  $\Phi_{\text{KS}}$ . The two different definitions lead naturally to different representations of the exchange term (local in KS, nonlocal in HF) in the corresponding single-particle equations.

In HF the nonlocal Fock exchange term acts in a different way on the occupied and on the virtual orbitals and this asymmetry can lead to counterintuitive and unphysical behaviour of the HF orbitals and their energies. For example, the virtual HF orbitals appear to be repelled by a charge of  $N$  rather than  $N - 1$  electrons[4], a fact that has led to the interpretation of the virtual orbital energies as (negative) electron affinities, in an obvious extension of Koopmans' theorem [5]. On the other hand, if we view that a virtual HF orbital represents an excitation of a ground state orbital, then the repulsion of the virtual orbital by a charge of  $N$  rather than  $N - 1$  electrons becomes a qualitative error arising from the self-repulsion of the occupied orbital – accommodating the electron before excitation – with the virtual orbital hosting to the electron after excitation. Ref.[6] discusses a similar case of self-repulsion (“ghost-interaction”) in ensemble DFT for excited states.

The self-repulsion of the virtual orbitals and the asymmetry of the action of the Fock operator on occupied and virtual orbitals leads to too high single-particle excitation energies and to poor band-structures with too large band gaps. In metals, the density of states of the uniform electron gas is found to vanish at the Fermi energy[7], predicting wrongly the behaviour of an ideal metal to be almost insulating. (However, see Ref. [8].) Another qualitative error of these spurious self-repulsions is that in unrestricted HF

theory there are no unfilled shells, i.e., the highest occupied and the lowest unoccupied orbitals are never degenerate, even in systems with odd number of electrons[9]. Finally, it seems counterintuitive that all the occupied HF orbitals turn out to have the same asymptotic decay[10].

The asymmetry in the HF treatment of occupied and virtual orbitals is well known and there is significant work to correct it, e.g. by making rotations in the Hilbert space of virtual orbitals[11]. An elegant solution to this problem is to employ a common, local, multiplicative, single-particle exchange potential  $\hat{v}_x = v_x(\mathbf{r})$ , that treats all orbitals, occupied and virtual, in a symmetric way. Indeed, with the self-interaction-free “exact exchange” (EXX) potential in KS theory (see Ref.[12] and references therein) single-particle properties, such as ionisation potentials[12, 15], electron affinities[12], single-particle excitation energies and band structures[12, 16, 17, 18] are obtained accurately. We note that the EXX potential cannot be written explicitly in terms of the electron density, but it must be obtained indirectly from the density, by solving a Fredholm integral equation of the first kind, known as the equation for the optimized effective potential (OEP) method [13, 14, 12]. In the terminology of KS theory, when correlation is omitted the EXX potential is also referred to as the exchange optimized effective potential (xOEP).

By comparison, in semi-local KS approximations (such as the local density approximation, LDA, and other related approximations) the cancellation of self-interactions is incomplete making the asymptotic decay of the exchange potential too fast, thus leading to inferior single-particle properties. In fact, the enforcement of the correct asymptotic behaviour is sufficient to improve considerably the accuracy of single-particle properties in these approximations [19].

Given that the exchange energy and exchange potential are not measurable quantities, the question arises about their dependence on the reference state of the effective model. For example, are there physical limits where this dependence can be expected to be either strong or weak? This question will be investigated in the following, after obtaining the local exchange potential (“local Fock exchange”, LFX) corresponding optimally to HF’s nonlocal Fock exchange term.

## 2. The local Fock exchange potential

The KS system is a virtual system of noninteracting electrons defined to have the same ground state charge density as the interacting system of interest. The KS system is determined by solving single-particle (KS) equations featuring the KS potential, which forces the noninteracting electrons to have the required density.

In DFT, the KS potential (functional derivative w.r.t. density of the noninteracting kinetic energy functional) is the sum of the electron-nuclear attraction,  $v_{\text{en}}(\mathbf{r})$ , the Hartree potential  $\int d\mathbf{r}' \rho(\mathbf{r}')/|\mathbf{r} - \mathbf{r}'|$ , and the exchange and correlation potential,  $v_{\text{xc}}(\mathbf{r})$ ; the latter is the functional derivative w.r.t. the density of the exchange and correlation energy. In particular the xOEP is the functional derivative of the exact exchange energy,

given by the Fock expression (1) in terms of the KS orbitals.

Ref. [20] gives an alternative (to DFT) and direct way to obtain ab initio approximations for the KS potential, by minimizing an appropriate energy difference ( $T_\Psi[v]$ , see the variational principle (4) in [20]). We note that the formalism in [20] assumes some knowledge of the interacting ground state  $\Psi$ . Also, we point out that although the theoretical scheme developed in Ref. [20], is based on wave function theory rather than DFT, it still results in the usual KS single-particle equations employing the (exact or approximate) KS potential.

In the following, to derive the local potential that best simulates the nonlocal Fock exchange term, we follow Ref. [20], and use the HF ground state Slater determinant  $\Phi_{\text{HF}}$  in place of the interacting state  $\Psi$ . Then, we search among all effective Hamiltonians  $H_v$  characterised by a local potential  $v(\mathbf{r})$ ,

$$H_v = \sum_{i=1}^N \left\{ -\frac{\nabla_i^2}{2} + v(\mathbf{r}_i) \right\}, \quad (2)$$

for the one ( $H_{v_{\text{MP0}}}$ ) which adopts optimally  $\Phi_{\text{HF}}$  as its own approximate ground state. The optimisation is achieved using the Rayleigh Ritz variational principle and minimising, over all local potentials  $v(\mathbf{r})$ , the non-negative energy difference,

$$T_{\text{HF}}[v] \geq 0, \text{ with } T_{\text{HF}}[v] \doteq \langle \Phi_{\text{HF}} | H_v | \Phi_{\text{HF}} \rangle - E_v. \quad (3)$$

$E_v$  is the ground state energy of  $H_v$ . The functional derivative of  $T_{\text{HF}}[v]$  is equal to the difference of the HF density and the density of the effective system [20],

$$\frac{\delta T_{\text{HF}}[v]}{\delta v(\mathbf{r})} = \rho_{\text{HF}}(\mathbf{r}) - \rho_v(\mathbf{r}). \quad (4)$$

At the minimum, the two densities are equal and the optimal potential  $v_{\text{MP0}}$  has the same density as HF. The difference of  $v_{\text{MP0}}$  and the sum of the Hartree potential and the electron-nuclear attraction defines the local Fock-exchange (LFX) potential:

$$v_{\text{LFX}}(\mathbf{r}) \doteq v_{\text{MP0}}(\mathbf{r}) - v_{\text{en}}(\mathbf{r}) - \int d\mathbf{r}' \frac{\rho_{\text{HF}}(\mathbf{r}')}{|\mathbf{r} - \mathbf{r}'|}. \quad (5)$$

Compared with the exchange optimised effective potential (xOEP) case, the functional derivative in (4) is easier to obtain, as it does not involve the calculation of the orbital shifts[18, 21].

The local potential with the HF density was studied in the past but also recently, in Ref. [22, 23], where it was found that it provides an almost perfect approximation to xOEP, avoiding mathematical issues in the implementation of xOEP with finite basis sets.

However, from our variational derivation we argue that LFX is actually more than a mere approximation to xOEP: both potentials are optimal in Rayleigh-Ritz energy minimizations where we search for the effective Hamiltonian  $H_v$  that, either adopts the HF ground state  $\Phi_{\text{HF}}$  optimally as its own approximate ground state (LFX), or, whose ground state minimizes the HF total energy (xOEP). In either case, if the restriction of a local potential were relaxed, the HF Hamiltonian would be the minimizing one.

It follows that both the LFX potential and the xOEP simulate optimally the nonlocal Fock exchange term in the HF single-particle Hamiltonian.

In the following we demonstrate that the xOEP and the LFX potential share other characteristic properties associated in the literature with exchange. For example, they both form zero-order terms in separate power series expansions of the KS potential, where the first order corrections vanish [24], as we show below.

At the variational derivation of  $v_{\text{MP}0}$  above, if in place of  $\Phi_{\text{HF}}$  we employed a finite-order expansion of the interacting ground state using Møller-Plesset (MP) Perturbation Theory (PT) [1], and then at each order performed the same optimisation, we would generate a corresponding MP series expansion for the KS potential. From Brillouin's theorem [1], singly excited Slater determinants do not couple directly with the HF ground state and so, the density of the MP ground state does not change from zero to first order. Hence, in the MP expansion of the KS potential, the zero-order term is  $v_{\text{MP}0}$  and the first-order correction vanishes. The same holds true for xOEP [25, 26] in DFT PT [27]: the sum of the xOEP, the Hartree potential and  $v_{\text{en}}$ , form the local potential in the zero-order effective Hamiltonian  $H_v$ , where, if we switch on electronic repulsion the electronic density will not change to first order. This result was re-derived in Ref. [20], using a general version of the variational principle (3).

Probably the most characteristic property of the exchange potential is that it is the functional derivative of the exchange energy (1) and as a consequence xOEP satisfies the virial relation for exchange:

$$E_x[\Phi_{\text{xOEP}}] + \int dr \rho(\mathbf{r}) \mathbf{r} \cdot \nabla v_{\text{xOEP}}(\mathbf{r}) = 0. \quad (6)$$

The LFX potential is not the functional derivative of the exchange energy, satisfying a different virial relation [24]:

$$E_x[\Phi_{\text{LFX}}] + \int dr \rho(\mathbf{r}) \mathbf{r} \cdot \nabla v_{\text{LFX}}(\mathbf{r}) + E_c^{\text{HF}} + T_c^{\text{HF}} = 0, \quad (7)$$

where,

$$T_c^{\text{HF}} \doteq \langle \Phi_{\text{HF}} | T | \Phi_{\text{HF}} \rangle - \langle \Phi_{\text{LFX}} | T | \Phi_{\text{LFX}} \rangle \quad (8)$$

$$E_c^{\text{HF}} \doteq \langle \Phi_{\text{HF}} | T + V_{\text{ee}} | \Phi_{\text{HF}} \rangle - \langle \Phi_{\text{LFX}} | T + V_{\text{ee}} | \Phi_{\text{LFX}} \rangle \quad (9)$$

$V_{\text{ee}}, T$  are the interaction and kinetic energy operators.

Consider now the perturbation treatment of the  $N$ -electron HF Hamiltonian, with zero order  $H_{v_{\text{MP}0}}$  (Eq. 2, with  $v = v_{\text{MP}0}$ ) and perturbation  $\hat{K} - \sum_i v_{\text{LFX}}(\mathbf{r}_i)$ ,

$$H_{\text{HF}} = H_{v_{\text{MP}0}} + \lambda \left( \hat{K} - \sum_i v_{\text{LFX}}(\mathbf{r}_i) \right), \quad (10)$$

where by  $\hat{K}$  we denote the many-body, nonlocal Fock exchange term. The zero order Hamiltonian and the perturbation are composed of one-body operators (both  $H_{\text{HF}}$  and  $H_{v_{\text{MP}0}}$  have similar Slater determinant eigenstates) and hence the perturbation expansion in powers of  $\lambda$  is expected to converge fast.

Since they share the same ground state density,  $H_{v_{\text{MP}0}}$  and  $H_{\text{HF}}$  can be connected with an adiabatic connection path along  $\lambda$ , for  $0 \leq \lambda \leq 1$  [28, 29, 30]. Then, following

Levy and Perdew [31] we obtain,  $E_c^{\text{HF}} + T_c^{\text{HF}} = 0$ , to second order in  $\lambda$ , and consequently *the LFX potential satisfies the virial relation for exchange (6) to second order* in this rapidly convergent expansion in  $\lambda$ . This explains the nearly perfect exchange-virial results in Ref. [22, 23].

We conclude that the difference between the xOEP and the LFX potential is analogous to the difference in the definitions of the exact exchange energy in wave function theory and in DFT. Although the two potentials are mathematically different, they describe the same physics and consequently we expect the results of calculations employing these two potentials to be similar, at least in systems where exchange dominates over correlation (weakly interacting).

### 3. Algorithm to construct the LFX potential

We now discuss our practical implementation method to calculate the LFX potential. The variational principle,  $T_{\text{HF}}[v] \geq 0$ , suggests the following steepest descent algorithm to determine the potential  $v_{\text{MPO}}$ :

- Start with a trial potential  $v$  that yields a ground state density  $\rho_v$ .
- If  $\rho_v \neq \rho_{\text{HF}}$ , correct the potential in the direction,

$$v(\mathbf{r}) \rightarrow v(\mathbf{r}) - \epsilon \int d\mathbf{r}' \frac{\rho_{\text{HF}}(\mathbf{r}') - \rho_v(\mathbf{r}')}{|\mathbf{r} - \mathbf{r}'|} \quad (11)$$

where  $\epsilon > 0$  is a small, positive real number.

- Recalculate  $\rho_v$  for the corrected potential  $v(\mathbf{r})$ .
- Iterate to convergence.

For  $\rho_v \neq \rho_{\text{HF}}$  and sufficiently small  $\epsilon$ , the change of the potential (11) reduces the energy difference in (3) by  $\epsilon U_{\rho_{\text{HF}}}[v]$ , where  $U_{\rho_{\text{HF}}}[v]$  is the Coulomb energy of the density difference  $\rho_{\text{HF}} - \rho_v$ :

$$U_{\rho_{\text{HF}}}[v] \doteq \int d\mathbf{r} d\mathbf{r}' \frac{[\rho_{\text{HF}}(\mathbf{r}) - \rho_v(\mathbf{r})][\rho_{\text{HF}}(\mathbf{r}') - \rho_v(\mathbf{r}')]}{|\mathbf{r} - \mathbf{r}'|} \geq 0 \quad (12)$$

The algorithm stops only when the two densities become equal, within a small computational tolerance. In practice a numerical optimization method, such as conjugate gradient, is used to accelerate convergence.

It can be shown that for small enough  $\epsilon$ , the change in (11) reduces also the Coulomb energy  $U_{\rho_{\text{HF}}}[v]$  in every iteration. In fact, the algorithm is general and for any target density  $\rho$ , the minimisation using (11) of  $U_\rho[v]$  (the Coulomb energy of the density difference  $\rho - \rho_v$ ), can be employed to invert  $\rho$  and obtain the minimising local potential with ground state density equal to  $\rho$ . For related algorithms, see Refs. [32, 33] and the discussion in [34, 35].

The functional derivative,  $\delta T_{\text{HF}}[v]/\delta v(\mathbf{r})$ , represents a charge density (4) with zero net charge (as does the functional derivative,  $\delta E[v]/\delta v(\mathbf{r})$ , of any energy expression  $E[v]$  that is a functional of a local potential  $v(\mathbf{r})$ ; the net charge,  $\int d\mathbf{r} \delta E[v]/\delta v(\mathbf{r})$ , vanishes because the potential is defined up to a constant).

The correction of the potential in (11) is in the opposite direction of the Coulomb

potential of that charge density. In Ref. [18] we had employed a different algorithm, where the potential was corrected in the opposite direction of the functional derivative,  $\delta E[v]/\delta v(\mathbf{r})$ , rather than the Coulomb potential of the functional derivative (see Fig. 1 in Ref. [18]). Here, the analogous algorithm to Ref. [18] would have been:  $v(\mathbf{r}) \rightarrow v(\mathbf{r}) - \epsilon[\rho_{\text{HF}}(\mathbf{r}) - \rho_v(\mathbf{r})]$ . We found that this algorithm too converges to the same LFX potential, but is less stable and suffers from slow convergence rate in regions of low density.

### 3.1. Implementation and Convergence

The LFX potential has been implemented in the electronic-structure, plane-wave code CASTEP [36, 37], using the algorithm described above. The procedure to calculate the LFX potential, requires first a HF calculation to determine the target density ( $\rho_{\text{HF}}$ ). The second ingredient is the initial trial potential  $v$ , for which we choose the LDA potential corresponding to the target density; we have tried other density-dependent potentials and they perform equally well. The rest of the LFX potential calculation proceeds iteratively: we solve the single-particle equations with the potential  $v(\mathbf{r})$  and obtain the occupied orbitals and their density  $\rho_v$ . The difference of the Coulomb potentials of the densities,  $\rho_{\text{HF}} - \rho_v$  (see Eq. 4), is used to correct the potential using (11) in a line search, where in the latter case,  $\epsilon$  is chosen to minimise  $U_{\rho_{\text{HF}}}[v]$ . This procedure gives a down-hill direction allowing implementation of a Fletcher-Reeved based conjugate gradients algorithm with a line search based on a parabolic two-step fit. The iterative procedure is repeated until both  $U_{\rho_{\text{HF}}}[v]$  and the change in  $U_{\rho_{\text{HF}}}[v]$  with each iteration become comparable or smaller than the threshold values of  $1\mu\text{eV}$  and  $\sim 0.01\mu\text{eV}$  respectively.

In plane-wave DFT implementations the orbitals, density, and potentials are represented on rectilinear grids. The Kohn-Sham orbitals are described within a sphere bounded by the cutoff wave vector,  $G_{\text{max}}$ , and the density and potentials are nonzero within a sphere of radius  $2G_{\text{max}}$ . The iterative optimisation scheme we developed is performed explicitly on these real space grids by direct variation, so that the effective basis used to represent  $v(\mathbf{r})$  is the set of grid points  $\{\mathbf{G}\} : |\mathbf{G}| \leq 2G_{\text{max}}$ .

In the calculations that follow, the basis set size (plane-wave cutoff energy) and Brillouin-zone sampling were chosen so that total energy differences, evaluated in xOEP, were less than 2.5 meV/atom.

### 3.2. Finite basis OEP errors and CEDA potential

The implementation of the OEP method involves the expansion of the orbitals and the potential in finite basis sets. This procedure may introduce spurious oscillations in OEP, caused by a discontinuity in the solution of the finite-basis OEP equations [38]. In practice, we find that with the large orbital basis sets we use, containing several thousands of plane-waves, this discontinuity is negligible. (The discontinuity of finite-basis OEP [38] is expected to diminish with increasing size of orbital basis [38, 39, 40].)

Table 1: Total energy differences  $\Delta E$  (in eV) from the HF energy and Kohn Sham bandgaps (in eV) for xOEP, LFX and CEDA potentials. Last column gives experimental bandgap values; from Refs. [18, 47].

	$\Delta E$			Band Gap				Exp.
	xOEP	LFX	CEDA	xOEP	LFX	CEDA		
Ge	0.432	0.441	0.724	0.91	0.91	0.39	0.79	
InN	0.467	0.480	0.700	1.36	1.32	0.73	0.93	
Si	0.213	0.213	0.299	1.18	1.18	0.71	1.16	
GaAs	0.428	0.444	0.718	1.89	1.85	1.00	1.52	
CdTe	0.390	0.397	0.572	2.22	2.16	1.57	1.61	
ZnSe	0.472	0.485	0.702	2.89	2.85	2.14	2.80	
GaN	0.401	0.416	0.652	3.29	3.27	2.65	3.39	
ZnO	0.381	0.391	0.539	3.49	3.41	2.88	3.43	
C	0.159	0.160	0.224	4.77	4.78	4.25	5.47	
CaO	0.258	0.264	0.546	6.08	5.93	4.73	8.97	
NaCl	0.050	0.050	0.112	6.28	6.23	5.47	7.09	
FeO	1.438	1.595	2.994	1.21	0.72	0.36	2.4	
CoO	1.595	1.698	3.193	2.26	1.95	1.11	2.5	
MnO	0.823	0.951	1.833	3.85	3.30	3.36	3.9	
NiO	1.647	1.717	3.403	3.93	3.74	2.72	4.0	

Finally, we implemented the “common energy denominator approximation” (CEDA) to xOEP [41]. CEDA is equivalent [42] to the “effective local potential” [43] and to the “localised Hartree Fock” potential [44]. These approximate xOEPs are related to the Krieger-Li-Iafrate (KLI) approximation [45], since they are all based on the Unsöld approximation [46].

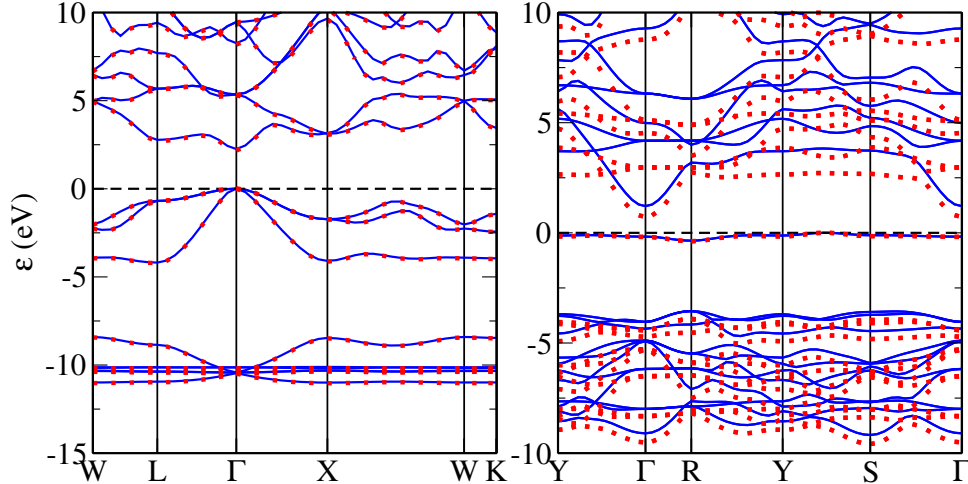
#### 4. Results

The differences in total energies, from the HF total energy, for the xOEP, LFX and CEDA potentials are shown in Table 1, for a selection of semiconductors, insulators and anti-ferromagnetic transition metal monoxides (TMOs). In every case we used the HF total energy expression in terms of the occupied orbitals of the corresponding potential. Also included in Table 1 are the Kohn-Sham band-gaps for each material, calculated as the difference between the conduction band minimum and valence band maximum. The values for the experimental bandgaps for the semiconductors and insulators are from Ref. [18] and references therein. The experimental bandgaps and magnetic moments (Tables 1, 2) for the TMOs are from Ref. [47] and references therein.

The calculations on the semiconductors and insulators used experimental lattice constants in the zincblende structure for Ge, Si, GaAs, CdTe, ZnSe, C, the wurtzite structure for InN, GaN and ZnO and the rocksalt structure for CaO and NaCl.

The HF energy is the lowest among all the methods due to the greater variational freedom of the orbitals compared to the local potential. The total energies corresponding

Figure 1: Band structures of CdTe (left) and FeO (right), blue solid lines are for xOEP and red dotted lines are for LFX. The blue and red lines are indistinguishable in CdTe but differ in FeO. The discrepancy indicates stronger correlations.



to the xOEP and LFX potentials are higher by 0.5 eV and within 15 meV of each other, with the largest difference observed in GaN. Of these the LFX energy is slightly higher, in accord with the definition of xOEP as the minimum among effective schemes with a local potential. As expected, the CEDA total energies are significantly higher. Band structures generated using the xOEP and LFX potentials are also very similar. A typical example, CdTe, is plotted in Figure 1, where the difference is undetectable. For materials not considered “highly correlated” the largest difference of 0.15 eV for CaO would be barely visible on the same scale. CEDA bandgaps are systematically smaller by between a few tenths of eV and 1 eV. Such close similarities support our contention that the xOEP and LFX potentials capture equally well the physics of the exchange term in the single-particle equations.

Our results agree well with EXX/xOEP results in the literature, showing that KS bandgaps (without a discontinuity correction) predict the fundamental bandgaps of semiconductors and insulators rather accurately, but with the quality of the agreement generally deteriorating with increasing width of the insulator bandgap [16, 17, 48, 12].

#### 4.1. Transition metal oxides

Calculations for the TMOs were performed in the experimental rocksalt structure without any rhombohedral distortion. The simulation cell was the primitive rhombohedral cell of the AFM II magnetic structure, which is consistent with antiferromagnetic order between alternating cubic (111) planes. All four methods (HF, xOEP, LFX, CEDA) predict the four materials to be antiferromagnetic insulators. The xOEP total energy is slightly below the LFX total energy, differing by at most 0.16eV for FeO (whose xOEP and LFX band structure is in Figure 1); both of these

Table 2: Magnetic moments (in  $\mu_B$ ) for transition metal monoxides for xOEP, LFX and CEDA. Experimental values from Ref. [47].

	xOEP	LFX	CEDA	Exp.
FeO	4.00	3.98	3.98	3.32, 4.2
CoO	2.98	2.94	2.90	3.35, 3.98
MnO	5.06	5.10	4.98	4.58, 4.79
NiO	1.92	1.90	1.80	1.64, 1.90

methods give energies very close to the HF minimum. As shown in Tables 1, 2, the exchange-only Kohn-Sham bandgaps and the calculated magnetic moments are close to the experimental values.

For the TMOs studied here, antiferromagnetism allows the opening of a gap in the single particle spectrum, although semi-local approximations (LDA/GGA) predict a gap that is too small or zero. The better treatment of self-interaction in hybrid functionals[49, 50], the Perdew-Zunger SIC[51], LDA+U [52], or previous EXX calculations[47] all yield improved agreement with experiment.

Our exchange-only results in TMOs are in good agreement with EXX results by Engel[47] which included LDA correlation. The close agreement between our exchange-only results and experiment suggests that the well-known failure of the semi-local LDA and GGA approximations is mainly due to the incomplete description of exchange rather than the strength of correlation [53].

However, it is well-known that the fundamental band-gap is not equal to the KS band-gap, and that the exchange and correlation discontinuity  $\Delta_{xc}$  must be added in order to obtain the correct value. The magnitude of  $\Delta_{xc}$  will decide if the accuracy of our exchange only results for the materials presented here (especially the TMOs) is a coincidence: if it is small, the description of these systems will be physically sound. In fact, if the intuition for the smallness of  $\Delta_{xc}$  at xOEP or LFX is verified, then, correlation in these results is not completely ignored, since it is included in the value of  $\Delta_{xc}$ .

## 5. Discussion

To conclude, we have presented a thorough study and comparison of two very similar but mathematically distinct local, single-particle, exchange potentials.

We applied our methods to a variety of systems, ranging from semiconductors, to wide-band insulators and to TMOs. For most systems, the results from the two calculations were very similar and almost indistinguishable. The main message of our paper is the robustness of our results, which bolsters confidence on the computational/numerical aspect of the results, since two entirely different calculations of the same underlying physical quantity turn out to agree in the end [54].

The results of the common energy denominator approximation (CEDA)

demonstrate the inferiority of the approximate treatment of exchange, compared with the more accurate treatment afforded by xOEP and LFX.

The larger differences between LFX and xOEP in some systems, especially the TMOs, suggests that correlation plays a more significant role in those systems. We argue that the disparity between LFX and xOEP can be taken as a measure of the strength of correlation, as in principle, there is no *a priori* guarantee that xOEP and LFX should give the same result. Only in materials where the XC energy is dominated by the exchange term would we expect the two methods to agree.

## Acknowledgments

T.W.H. acknowledges the Engineering and Physical Sciences Research Council (EPSRC) for financial support, the UK national supercomputing facility (Archer), Durham HPC (Hamilton), the facilities of N8 HPC, provided and funded by the N8 consortium and EPSRC (Grant No. EP/K000225/1) and finally the UK Car-Parrinello Consortium for support under Grant No. EP/F037481/1.

- [1] Szabo A, and Ostlund NS, *Modern Quantum Chemistry*. (*Macmillan Publishing Co, Inc, New York*) (1996).
- [2] Kohn W, and Sham LJ, *Phys Rev* **140**, A1133-A1138 (1965).
- [3] Hohenberg P, and Kohn W, *Phys Rev* **136**, B864-B871 (1964).
- [4] Davidson ER, *Rev Mod Phys* **44**, 451-464 (1972).
- [5] Koopmans T, *Physica*, **1**, 104-113 (1934)
- [6] Gidopoulos NI, Papaconstantinou PG, and Gross EKU, *Phys Rev Lett* **88**, 033003 (2002).
- [7] Ashcroft NW, and Mermin ND, *Solid State Physics*, Saunders College Publishing, Harcourt, Inc., Orlando, (1976).
- [8] Blair AI, Kroukis A, Gidopoulos NI, *J Chem Phys* **142**, 084116 (2015); doi: 10.1063/1.4909519
- [9] Bach V, Lieb EH, Loss M, and Solovej JP, *Phys Rev Lett* **72**, 2981-2983 (1994).
- [10] Handy NC, Marron MT, and Silverstone HJ, *Phys Rev* **180**, 45-48 (1969).
- [11] Davidson ER, *J Chem Phys* **57**, 1999-2005 (1972).
- [12] Kümmel S, and Kronik L, *Rev Mod Phys* **80**, 3-60 (2008).
- [13] Sharp RT, and Horton GK, *Phys Rev* **90**, 317-317 (1953).
- [14] Talman JD, and Shadwick WF, *Phys Rev A* **14**, 36-40 (1976).
- [15] Görling A, *Phys Rev Lett* **83**, 5459-5462 (1999).
- [16] Städele M, Majewski JA, Vogl P, and Görling A, *Phys. Rev. Lett.* **79**, 2089, (1997)
- [17] Städele M, Moukara M, Majewski JA, Vogl P, and Görling A, *Phys. Rev. B* **59**, 10031, (1999)
- [18] Hollins TW, Clark SJ, Refson K, and Gidopoulos NI, *Phys Rev B* **85**, 235126 (2012).
- [19] Gidopoulos NI, and Lathiotakis NN, *J Chem Phys* **136**, 224109 (2012).
- [20] Gidopoulos NI, *Phys Rev A* **83**, 040502(R) (2011).
- [21] Kümmel S, and Perdew JP, *Phys Rev Lett* **90**, 043004 (2003).
- [22] Ryabinkin IG, Kananenka AA, and Staroverov VN, *Phys Rev Lett* **111**, 013001 (2013).
- [23] Kohut SV, Ryabinkin IG, Staroverov VN, *J. Chem. Phys.* **140**, 18A535 (2014)
- [24] Gidopoulos NI, to be published.
- [25] Bartlett RJ, Lotrich VF, Schweigert IV, *J. Chem. Phys.* **123**, 062205 (2005).
- [26] Görling A, and Levy M, *Int J Quantum Chem: Quantum Chemistry Symposium* **29**, 93-108 (1995).
- [27] Görling A, and Levy M, *Phys. Rev. B* **47**, 13105 (1993)
- [28] Langreth DC and Perdew JP, *Solid State Commun* **17**, 1425 (1975); *ibid Phys. Rev. B* **15**, 2884 (1977).
- [29] Gunnarsson O, and Lundqvist BI, *Phys. Rev. B* **13**, 4274 (1976).

- [30] Harris J, and Jones RO, *J. Phys. F* **4**, 1170 (1974)
- [31] Levy M, Perdew JP, *Phys Rev A* **32**, 2010 (1985)
- [32] Wu Q, and Yang W, *J Chem Phys* **118**, 2498-2509 (2003).
- [33] Peirs K, Van Neck D, Waroquier M, *Phys Rev A* **67**, 012505 (2003)
- [34] Baerends EJ, Gritsenko O, *J. Chem. Phys.* **145**, 037101 (2016); doi: 10.1063/1.4958622
- [35] Ryabinkin IG, Kohut SV, Cuevas-Saavedra R, Ayers PW, Staroverov VN, *J. Chem. Phys.* **145**, 037102 (2016); doi: 10.1063/1.4958623
- [36] Segall MD, Lindan PJD, Probert MJ, Pickard CJ, Hasnip PJ, Clark SJ, and Payne MC, *J Phys: Condens Matter* **14**, 2717-2744 (2003).
- [37] Clark SJ, Segall MD, Pickard CJ, Hasnip PJ, Probert MJ, Refson K, and Payne MC, *Z. Kristallogr* **220**, 567-570 (2005).
- [38] Gidopoulos NI, and Lathiotakis NN, *Phys Rev A* **85**, 052508 (2012)
- [39] Friedrich C, Betzinger M, and Blügel S, *Phys Rev A* **88**, 046501 (2013).
- [40] Gidopoulos NI, and Lathiotakis NN, *Phys Rev A* **88**, 046502 (2013).
- [41] Grüning M, Gritsenko OV, and Baerends EJ, *J Chem Phys* **116**, 6435-6442 (2002).
- [42] Bulat FA, and Levy M, *Phys Rev A* **80**, 052510 (2009).
- [43] Staroverov VN, Scuseria GE, and Davidson ER, *J Chem Phys* **125**, 081104 (2006).
- [44] Della Sala F, and Görling A, *J Chem Phys* **115**, 5718-5732 (2001).
- [45] Krieger JB, Li Y, and Iafrate GJ, *Phys Rev A* **46**, 5453-5458 (1992).
- [46] Unsöld A, *Z Phys* **43**, 563-574 (1927).
- [47] Engel E, Schmid RN, *Phys Rev Lett* **103**, 036404 (2009).
- [48] Magyar RJ, Fleszar A, Gross EKU, *Phys. Rev. B* **69**, 045111 (2004)
- [49] Cora F, Alfredsson M, Mallia G, Middlemiss D, Mackrodt WC, Dovesi R, and Orlando R, *Structure and Bonding*, **113**, 171-232 (2004).
- [50] Clark SJ, and Robertson J, *Physica Status Solidi (B)*, **248**, 537-546 (2011).
- [51] Dane M, Luders M, Ernst A, Kodderitzsch D, Temmerman WM, Szotek Z, and Hergert W, *J. Phys. Condens. Matter* **21**, 045604 (2009).
- [52] Anisimov VI, Zaanen J, and Andersen OK, *Physical Review B* **44**, 943-954 (1991).
- [53] Betzinger M, Friedrich C, and Blügel S, *Phys Rev B* **88**, 075130 (2013)
- [54] Lejaeghere K, *et al* *Science* **351** 1415 (2016).